Atmos. Chem. Phys. Discuss., https://doi.org/10.5194/acp-2018-183
Manuscript under review for journal Atmos. Chem. Phys.
Discussion started: 9 March 2018

Concentration, temporal variation and sources of black carbon in the Mount Everest region retrieved by real-time observation and simulation

Xintong Chen [1, 4], Shichang Kang [1, 2, 4], Zhiyuan Cong[2, 3], Junhua Yang [1], Yaoming Ma [3]

[1]State Key Laboratory of Cryospheric Science, Northwest Institute of Eco-Environment and Resources, Chinese Academy of Sciences, Lanzhou 730000, China

[2]CAS Center for Excellence in Tibetan Plateau Earth Sciences, Chinese Academy of Sciences, Beijing, 100101, China

[3]Key Laboratory of Tibetan Environment Changes and Land Surface Processes, Institute of Tibetan Plateau Research, Chinese Academy of Sciences, Beijing 100101, China

[4]University of Chinese Academy of Sciences, Beijing 100049, China.

Correspondence to: Shichang Kang (shichang.kang@lzb.ac.cn)

Abstract. Based on the high-resolution measurement of black carbon (BC) at Qomolangma (Everest) station of Chinese Academy of Sciences during 15 May 2015 to 31 May 2017, we investigated the seasonal and diurnal variations of BC and its potential source regions. Monthly and daily mean BC concentrations reached the highest values in the pre-monsoon season which are at least one magnitude higher than the lowest values in the monsoon season. For the diurnal variation, BC concentrations were significantly greater from mid-night to noon in the pre-monsoon season and showed increasing trend in the afternoon in the non-monsoon seasons, implying the potential contribution from the long-range transport. In the monsoon season, BC concentrations appeared two peaks in the morning and after the noon, might be affected by the local anthropogenic activities. By analyzing the simulation results from the backward air-mass trajectories and the fire spots distribution from the MODIS data, we found that the seasonal cycle of BC was significantly influenced by atmospheric circulation and combustion intensity in the Mt. Everest region. The transport mechanisms of BC were revealed using WRF-Chem simulation during severe pollution episodes. For the pollution event in the monsoon season, BC aerosols in South Asia could be uplifted and transported to the Mt. Everest region by the southward winds in the upper atmosphere. However, for the events in the pre-monsoon season, BC from northern India was brought and concentrated in the southern slope of the Himalayas by the northwesterly winds in the lower atmosphere and then transported across the Himalayas by the mountain-valley wind, while relatively less BC from northwestern India and Central Asia could be transported to the Mt. Everest region by the westerly winds in the upper atmosphere.

1 Introduction

Black Carbon (BC), from the incomplete combustion of fossil fuels or biomass burning, has drawn lots of attention due to its influences on environment and human health (Anenberg et al., 2012; Bond, 2004; Ramanathan et al., 2005), and is seen as an important factor that may lead to global warming besides greenhouse gases (Hansen et al., 2000; Jacobson, 2002; Bond et al., 2013). BC can greatly absorb solar radiation and causes atmosphere heating (Jacobson, 2001; Ramanathan et al., 2005;

Ji et al., 2015). Moreover, BC as fine particles can suspend in the atmosphere for about one week and transports far away from its emission sources, and be removed by dry and wet deposition (Oshima et al., 2012; Cooke et al., 2002; Jurado et al., 2008). When BC deposited on snow and ice, it can significantly reduce surface albedo and accelerate glacier and snow cover melting, causing the impact on regional climate, hydrology, and water resources (Ming et al., 2008; Li et al., 2018; Ramanathan and Carmichael, 2008).

The Tibetan Plateau (TP), generally known as the "Third Pole", is the highest plateau with a large number of glaciers and snow cover (Kang et al., 2010; Lu et al., 2010; Yao et al., 2012). Even though the TP is remote region with little affected by anthropogenic activities, previous observations have indicated that BC is an important contributor to the rapid shrinking of glaciers over the TP via decreasing surface albedo and atmospheric warming (Xu et al., 2009; Yang et al., 2015; Yasunari et al., 2010; Li et al., 2017; Zhang et al., 2017b; Qu et al., 2014; Ji, 2016; Xu et al., 2016). Moreover, previous studies have also suggested that the emissions from South Asia and East Asia are the major sources of BC in the TP (Lu et al., 2012; He et al., 2014; Zhang et al., 2015; Yang et al., 2018), and the high emissions from South Asia can across the Himalayas and further transport to the inland of the TP (Luthi et al., 2015; Xu et al., 2014; Cong et al., 2015a; Kang et al., 2016; Wan et al., 2015). Meanwhile, seasonality of BC aerosols are closely related to atmospheric circulation that helps to bring the BC aerosols across the Himalayas (Cong et al., 2015a; Yang et al., 2018; Zou et al., 2008). Additionally, a large number of studies have also demonstrated that the BC and dust from Central Asia and Northern Africa could also be transported to the TP (Wang et al., 2016; Lu et al., 2012; Zhao et al., 2012; Wu et al., 2010; Zhang et al., 2015).

Mt. Everest could be regarded as the very sensitive area under the influence of BC aerosols. Previous research on atmospheric BC in the Mt. Everest region was mainly based on thermal/optical analytical method, using quartz filter samples (Cong et al., 2015a). However, investigating in diurnal and seasonal variations of BC still lacks in the region. Therefore, to fulfill such gaps and understand the variations and sources of BC in the pristine region, there is a need for an efficient approach and studies. The aethalometer can provide high-resolution and continuous real-time observation data on BC concentration which is very important and necessary to better depict the characteristics of BC and its effects on the environmental change.

In comparison with the observation, the numerical model can better represent the atmospheric physical and chemical processes. Many studies have used global climate models (GCMs) and chemical transport models (CTMs) to investigate the origin and transportation of BC over the TP (Lu et al., 2012; Zhang et al., 2015; Menon et al., 2010; Kopacz et al., 2011). However, due to the coarse resolution, it is difficult for the CTMs and GCMs to capture the surface details of the TP (Ji et al., 2015; Gao et al., 2008). Regional climate models (RCMs) can compensate for the shortcomings of coarser global model grids by the high-resolution simulations. In the recent decades, RCMs have been developed to include multiple modules and atmospheric chemistry processes. Also the advanced regional climate-chemistry model, Weather Research and Forecasting (WRF) model (Skamarock et al., 2005); with Chemistry (WRF-Chem), has been successfully applied for air quality research in the TP region (Yang et al., 2017; Yang et al., 2018).

Here, we present real-time data of BC concentration measured by the new generation aethalometer (AE-33), from 15 May 2015 to 31 May 2017. The observed results are used to characterize the temporal variation and provide the solid information on the possible sources and transport mechanism of BC. Combined high-resolution measurement of BC concentration and WRF-Chem model, we investigated the concentration level, temporal variation, and sources of BC in the Mt. Everest region. The purpose of this study is to understand the impact of trans-boundary atmospheric BC on the Mt. Everest region and depict the transport pathways of BC in different spatiotemporal scales.

2 Materials and methods

2.1 Sampling site and meteorological condition

Mt. Everest (27.98°N, 86.92°E, 8844 m a.s.l.), the summit of the world, is located in the central Himalayas. The southern slope of the Mt. Everest is adjacent to the Indian continent, and the climate is warm and humid under the influence of the Indian summer monsoon. Conversely, the northern side is cold and dry since the warm and humid airflow cannot reach there. The Qomolangma Atmospheric and Environmental Observation and Research Station (QOMS, 28.36°N, 86.95°E, 4276 m a.s.l.) of Chinese Academy of Sciences (Fig. 1) is located in the northern slope of the Mt. Everest, which was established for the continuous monitoring of atmospheric environment (Cong et al., 2015a; Ma et al., 2011).

The meteorological parameters, i.e., air temperature, air pressure, humidity, wind speeds and wind direction, were recorded by an automatic weather station at QOMS. Meanwhile, the precipitation data were collected by artificial measurement, as shown in Fig. 2. The entire year was divided into four seasons according to the Indian monsoon transitions characteristics, which includes pre-monsoon (March to May), monsoon (June to September), post-monsoon (October to November), and winter (December to February) (Praveen et al., 2012; Zhang et al., 2017a). A clear seasonal cycle of temperature and humidity could be observed from Fig. 2. Specifically, higher temperature was observed during the monsoon season while lower during winter, with a maximum in July and a minimum in January. Humidity followed the similar trend, with higher values from late July to early August and lower values from December to February. During the observation period, the wind speed increased significantly from November to April. The wind direction at QOMS is affected by the local topography that with series of small valleys. During the pre-monsoon season (Dry-period), the westerly and southerly winds begin to develop and play the important role in atmospheric pollution circulation. However, during the monsoon season, southwesterly winds prevail and bring much moisture from the Indian Ocean to the Mt. Everest region increasing the humidity and precipitation. With the retreat of monsoon, southwesterly winds decrease and the popular wind direction changes to westerly and northeasterly in winter with limited moisture (Fig. 2).

2.2 BC measurements

The airborne BC concentrations at QOMS were monitored by the "Next Generation" aethalometer model AE-33 (Magee Scientific Corporation, USA). The instrument was set in an indoor room with inlet installed at about 3 m above the ground level and was operated at an airflow rate of 4 LPM with 1 min time resolution at QOMS.

AE-33 has seven fixed wavelengths (i.e., 370，470，520，590，660，880 and 950 nm), which can acquire BC concentration according to light absorption and attenuation characteristics from the different wavelengths (Hansen et al., 1984; Drinovec et al., 2014). Generally, BC concentration measured at 880 nm is used as the actual BC concentration in the atmosphere, as the absorption of other species of aerosols is greatly reduced in this wavelength (Sandradewi et al., 2008a; Sandradewi et al., 2008b; Fialho et al., 2005; Yang et al., 2009; Drinovec et al., 2014). Compared to previous aethalometers, AE-33 uses doulspot method and a real-time calculation of the "loading compensation parameter", which can compensate for the "spot loading effect" and obtain high quality BC concentration (Drinovec et al., 2014). The algorithm is as follows:

$$BC\ (reported)=BC(zero\ loading)\times(1-kATN) \quad (1)$$

$$ATN=-100\ \ln(I/I_0) \quad (2)$$

$$BC1=BC\times(1-kATN1) \quad (3)$$

$$BC2=BC\times(1-kATN2) \quad (4)$$

Where, BC (reported) is the non-compensated BC concentration; BC (zero loading) is the desired ambient BC value that would be obtained in the absence of any loading effect; k is the loading compensation parameter; I and I_0 are the light intensity of the measurement spot and reference spot; ATN is the attenuation coefficient. BC component of aerosols is analyzed on two parallel spots drawn from the same input stream in AE-33, but collected at different rates of accumulation. It means that we can obtain different ATN but the same loading parameter k (Drinovec et al., 2014). Combining Eq. (3) and Eq. (4), the "loading compensation parameter" k and the desired value of BC compensated back to zero loading can be calculated.

2.3 Model simulation and datasets

The WRF-Chem version 3.6 was used to analyze the spatial distribution, transport mechanism, and source apportionment of BC during the four observed pollution episodes. The WRF-Chem model is the expansion of WRF meteorological model and considers complex physical and chemical process such as the emission and deposition, advection and diffusion, gaseous and aqueous chemical transformation, and aerosol chemistry and dynamics (Grell et al., 2005). Here, the numerical experiments were performed at 25 km horizontal resolution with 122 and 101 grid cell in the west-east direction and north-south, respectively. The simulated domain was centered at 25°N, 82.5°E and had a 30-layer structure with the top pressure of 50 hPa. Key physical and chemical parameterization options for the WRF-Chem modeling were according to the previous study in the TP (Yang et al., 2018). The initial meteorological fields were from National Centers for Environmental Prediction (NECP) reanalysis data with a horizontal resolution of 1 ° × 1 ° at 6-h time intervals. The anthropogenic emission inventory was obtained from the Intercontinental Chemical Transport Experiment-Phase B (INTEX-B) (Zhang et al., 2009) with a

resolution of 0.5° × 0.5°. The biogenic emissions were from the Model of Emission of Gases and Aerosol from Nature (MEGAN), and the fire emissions inventory was based on the fire inventory from NCAR (FINN) (Wiedinmyer et al., 2011). Additionally, the Model for Ozone and Related chemical Tracers (MOZART, http://www.acom.ucar.edu/wrf-chem/mozart.shtml) (Emmons et al., 2010) dataset were used to create improved initial and boundary conditions for BC simulations during these pollution episodes.

Furthermore, predicting the source region of BC, we used HYSPLIT-4 model to calculate the backward trajectories of air masses, and the data for calculation were from National Centers for Environmental Prediction/National Center for Atmospheric Research（NCEP/NCAR）data (2.5 ° × 2.5 °, 17 vertical levels). The active fire product provided by Fire Information for Resource Management System (FIRMS, https://firms.modaps.eosdis.nasa.gov/firemap/), was chosen to investigate the biomass burning emissions over the region in different seasons.

3. Results and discussion

3.1 Temporal variations of BC

3.1.1 Monthly variation of BC

Monthly mean BC concentrations at QOMS is shown in Fig. 3a. There was a significant increase in BC concentrations in winter and the highest value occurred during the pre-monsoon season (923.1 ± 685.8 ng/m^3 in April). Meanwhile, during monsoon, the lower BC concentrations were recorded and the lowest value was observed in July (88.5 ± 29.8 ng/m^3). This seasonal change was consistent with the previous studies of element carbon (EC or BC) at Nepal Climate Observatory-Pyramid station (NCO-P, 27.95°N, 86.82°E, 5079m a.s.l.) (Fig. 3b) (Marinoni et al., 2010) and at QOMS (Fig. 3c) (Cong et al., 2015a), indicating that the similar BC source between the southern and northern sides of the Himalayas. As the EC was sampled by the quartz filters and detected using the thermal/optical analytical method in the previous studies, there may have been some disparities in the values of EC with these of BC. The monthly variation of EC at Nam Co Monitoring and Research Station for Multisphere Interactions (Nam Co station, 30.46°N, 90.59°E, 4730 m a.s.l.) (Fig. 3d) (Wan et al., 2015) also showed the similar variation, but the peak value of EC occurred in winter. Additionally, monthly mean EC concentrations at Nam Co station were generally lower than that at QOMS, suggesting that anthropogenic activities impacts in the inland TP were weaker than that in the south edge of the TP. Previous studies have demonstrated that the influence of polluted air masses from the “Atmospheric Brown Clouds” over South Asia could reach to the southern foothills of the Himalayas, and the mountain-valley breeze circulation carried the polluted air masses onto the TP (Luthi et al., 2015; Cong et al., 2015a; Bonasoni et al., 2008; Yang et al., 2018). Therefore, the seasonal cycle of BC concentrations at QOMS was likely affected by the atmospheric circulation and the emissions from South Asia, and these will be further explained in Section 3.3.

3.1.2 Daily variation of BC

Fig. 4 shows the daily mean BC concentrations at QOMS which presents a significant seasonal pattern, with a maximum during the pre-monsoon season (2772.3 ng/m^3) and a minimum during the monsoon season (36.4 ng/m^3). During the monsoon season, BC concentration was observed to be lower than 150 ng/m^3, but it gradually increased during the post-monsoon and winter. The mean concentration of daily BC at QOMS was 298.8 ± 341.3 ng/m^3, which was close to the previous result (250 ± 220 ng/m^3) (Cong et al., 2015a). Such a result demonstrates that our results are consistent with the previous finding and systematic sampling of aerosol is also important to obtain BC values in the region.

The comparison between daily mean BC concentrations (Fig. 4) and the meteorological parameters (Fig. 2) suggested that the increasing humidity and precipitation during monsoon led to washout of atmospheric particles promoting the wet deposition of BC. This process caused a decrease in BC concentrations during monsoon representing the background level during the period. The prevailing wind direction during the monsoon period was southwesterly while in non-monsoon was dominated by westerly. Therefore, the variations of BC might be linked to the influence of meteorological conditions and the contribution of long-distance transport from urbanized areas to QOMS. Moreover, it cannot be ignored that there were continuous high concentrations of BC above 1000 ng/m^3 during 8-10 June 2015, 19-22 March 2016, 9-18 April 2016, and 11-14 April 2017, indicating the heavy pollution episodes happened at QOMS during those days. The detailed analysis for these pollution events is presented in Section 3.4.

3.1.3 Diurnal variation of BC

Diurnal variation characteristics can be used to analyze the impact of local meteorological process and anthropogenic activities on BC concentrations at QOMS. The half-hourly mean BC concentrations are presented in Fig. 5. The diurnal BC concentrations in the pre-monsoon season were significantly higher than those in other seasons, and remained high values from mid-night to noon and increased gradually after the lowest value around 15:00. The similar increasing trend for BC was observed in the afternoon mostly during the post-monsoon and winter periods, and highest BC concentration occurred from mid-night to noon. During the monsoon season, the BC concentrations remained low values with two peaks in the morning and after the noon, respectively. Previous studies have demonstrated that the local wind system in the northern slope of the Mt. Everest were composed by a morning “valley wind”, a late morning-afternoon ‘‘glacier wind’’ weakened by ‘‘valley wind’’, and an evening-early night “mountain wind’’(Zou et al., 2008). The QOMS is located in the s-shape valley north of the Mt. Everest (Ma et al., 2011). The down mountain wind or glacier wind from south developed in the afternoon and at night, which provided the potential possibility for pollutants from long-distance source transported to QOMS along the valley and enable the increase of BC concentrations in the non-monsoon periods. The valley wind from north in the morning, could bring the short-distance emissions from local cooking or heating to QOMS. BC concentrations appeared two peaks in the morning and after the noon in the monsoon season, which might be owing to the surrounding local emissions.

To explain the significant high values during mid-night to noon in the pre-monsoon season, the wind direction frequency

at QOMS during 0:00-12:00 and 12:00-24:00 are presented in Fig. 6. During the sampling period in the pre-monsoon season, W (west) winds prevailed from mid-night to noon (Fig. 6a), accounting for 18.1% of the total wind directions, followed by ENE (east-northeast) winds (16.4%). It is consistent with the discussion above that there exists potential impacts on BC concentrations at QOMS from long-distance human activity emissions, which can be carried by westerly winds, i.e., down mountain winds (Cong et al., 2015b). Moreover, the WRF-Chem simulation results showed that, the profile of equivalent potential temperature (EPT) increased with altitude and the planetary boundary layer height (PBLH) and wind speed were much lower from mid-night to noon (Fig. S1), indicating a more stable atmosphere that obstructs the diffusion of BC aerosols. While ESE (east-southeast) and NE (northeast) winds prevailed from noon to mid-night (Fig. 6b), accounting for 17.6% and 15.3% of total wind directions, respectively. Several villages are located easterly (around 5 km away) from QOMS thus lower BC values might reflect the short-distance emission sources.

3.2 Comparison of BC concentrations with other sites in the TP

In order to better understand the BC loading level, we compared our results with previous studies from other locations over the TP. As listed in Table 1, BC concentrations on Muztagh Ata Mountain and Qilian Mountain presented lower values, which can be regarded as the background concentration level for inland Asia (Zhao et al., 2012; Cao et al., 2009). In contrast, observed BC concentrations at QOMS were relatively higher than other remote locations in the TP, which has an increasing trend from the southern edge of the TP to the inland TP. Such as Nam Co and Ranwu, sites are isolated from anthropogenic activities with relatively clean atmospheric environments, but BC concentration at these two sites is recorded up to 130 ng/m^3, which may be likely due to the influence of long-range transport from South Asia (Wan et al., 2015; Wang et al., 2016). Compared with locations in the southern slope of the Himalayas (e.g., NCO-P and Manora Peak), the BC concentration at QOMS was close to that at NCO-P, but much lower than that at Manora Peak, which is near to the polluted areas in South Asia, and largely affected by anthropogenic emissions (Marinoni et al., 2010; Ram et al., 2010). It implied that combustion emissions from South Asia not only can affect the lower latitudes in the vicinity, but also can be transported to the higher latitudes in the Himalayas and even to the TP. However, the BC concentration at Lhasa city was higher than other remote sites in the TP, which was mainly from the local vehicle emissions (Li et al., 2016). But for BC concentration at Qinghai Lake, it was higher than that at the other south sites in the TP, because of the long-range transport of higher anthropogenic emissions from easterly and significant input from westerly (Li et al., 2013). On the whole, the BC concentrations over the TP varies with atmospheric circulation and upwind emission sources, and the high level of BC at QOMS suggest the significant influence of anthropogenic emissions from South Asia.

3.3 Potential sources and transport mechanism of BC in different seasons

The seasonal variation of BC concentrations was correlated with combustion intensity of sources and atmospheric

circulation. The "Atmospheric Brown Clouds" over South Asia contains large amounts of aerosol components such as the high loading emissions of BC from biomass burning, which can reach the TP within a few days (Ramanathan et al., 2005; Luthi et al., 2015; Ramanathan and Ramana, 2005). Previous study has quantified biomass burning source contributing to BC aerosols in the Himalayas, and showed that the major fires were concentrated in March to June, besides, most vegetation fires occurred in the low elevation areas in South Asia and were mainly from croplands and forests (Vadrevu et al., 2012). Therefore, we further checked the biomass burning emissions in the Mt. Everest region and its vicinities using the active fire product from the MODIS data at four seasons (August 2015 to April 2016) provided by the FIRMS (Fig. 7). It is clearly understood that there were large numbers of active fire spots in northern and central India, also in Pakistan and Nepal in winter and the pre-monsoon season, indicating that the agricultural combustion and forest fires contributed much to BC aerosols. During the monsoon season, no active fire spots distributed in South Asian region, representing the low biomass burning in that period.

To further explore the sources and the long-range transport mechanism of BC aerosols at QOMS, we calculated the frequency plots for 5-day backward trajectories arriving 1 km above the ground level (Fig. 8). During the non-monsoon seasons, air masses were affected by the westerly winds. The air masses reaching the Mt. Everest region were mostly from the northwest, indicating that the biomass burning emissions in Pakistan, northern Indian and Nepal could be transported to the Mt. Everest region. But for the difference of combustion intensity, the high concentrations of BC were found only during the pre-monsoon season. During the monsoon season, the southerly winds dominated in the Mt. Everest region and the air masses were mainly from the Arabian Sea and the Bay of Bengal with lots of moisture. At this period, the precipitation in the southern side of the Himalayas was above 1200 mm (Xu et al., 2014), which can improve the wet removal efficiency of BC. Moreover, the biomass combustion emissions in South Asia during this period were very low. Therefore, BC concentrations at QOMS were close to the background level during the monsoon season. Meanwhile, the local meteorological conditions also play a very important role in the transport of pollutants across the Himalayas from South Asia. Previous studies have shown that the local wind system was mainly composed by the uplift surface heating wind in the southern slope and downward glacier wind in the northern slope, which facilitates the exchange of air between bottom and upside of the atmosphere, also facilitates the coupling of airflow between the southern and northern slopes, which allows the pollutants from South Asia cross the Himalayas and transport to the TP from valley easily (Cong et al., 2015b; Zou et al., 2008; Tripathee et al., 2017; Chen et al., 2012; Dhungel et al., 2018).

3.4 Pollution episodes analysis by WRF-Chem modeling

In this section, we analyzed four pollution events with BC concentrations above 1000 ng/m^3 in detail, including event A during 8-10 June 2015, event B during 19-22 March 2016, event C during 9-18 April 2016, and event D during 11-14 April 2017. Fig. 9 shows the spatial characteristic of the WRF-Chem modeled surface BC concentrations during the four pollution episodes. It can be seen that, the high values of surface BC concentrations always appeared in South Asia, although the high-

value centers changed in different pollution events. For event A, the most serious pollution appeared in Nepal and northern India. Relatively, there were less BC nearby the Mt. Everest in event B. However, for event C, the high-value areas for BC concentrations were mainly along the southern slope of the Himalayas in Nepal and in the east of India, which can result in a great impact for BC concentrations in the Mt. Everest region. In event D, the high BC occurred in Nepal and some parts of India.

The sources and transport mechanism of BC aerosols during these pollution episodes can be indicated by analyzing the air flow. Fig. 10 shows the variation of BC concentrations and wind field at different altitudes in the atmosphere (850 hPa, 500 hPa, 200 hPa). For event A during the monsoon season, there was a cyclone in northern India at 850 hPa, which moved near-surface BC aerosols upward and then transported to the Mt. Everest region by the southward winds at 500 hPa and 200 hPa. For events B-D in the pre-monsoon season, northwesterly winds prevailed in South Asia at 850 hPa and brought BC from northern India to the southern slope of the Himalayas, and westerly winds at 500 hPa and 200 hPa can transport relatively less BC from northwestern India and Central Asia to the Mt. Everest region. Previous studies also pointed out that BC can be transported across the Himalayas to the Mt. Everest region by the mountain-valley wind system (Zou et al., 2008; Cong et al., 2015b; Dhungel et al., 2018). Thus, we needed to further analyze the impact of the mountain-valley wind on the transportation of BC. Fig. 11 shows the vertical profile of BC concentration among the QOMS's longitude of 86.95°E. During event A, high concentrations of BC appeared in the upper atmosphere of South Asia and many BC aerosols were transported to most parts of the TP (Fig. 11a), due to the large-scale transport process. However, for events B-D, high concentrations of BC occurred along the southern slope of the Himalayas and BC aerosols were only transported to a few areas of the northern slope of the Himalayas such as the Mt. Everest region (Fig. 11b-d), caused by the local mountain-valley wind. As shown in Fig. S2, for events B-D, the mountain wind in the southern side of the Himalayas can move BC aerosols up in the daytime and the down valley wind can make it fall down in the Mt. Everest region at night.

To sum up, we found that the transport processes of BC aerosols from South Asia to the QOMS were different as seasons varying. In the monsoon season such as event A, BC aerosols were moved upward by the cyclone in the lower atmosphere and were transported to QOMS by the southward winds in the upper atmosphere. However, in the pre-monsoon season such as events B-D, the mountain-valley wind played an import role in the BC aerosols transported from the southern slope of the Himalayas to the Mt. Everest region.

4. Conclusions

In this study, BC concentrations were measured from 15 May 2015 to 31 May 2017 at QOMS in the south edge of the TP, and monthly, daily, and diurnal variation of BC concentrations were calculated to investigate the temporal characteristics and potential sources of BC at QOMS. The results showed that the monthly mean BC concentrations reached the highest value in the pre-monsoon season (923.1 ± 685.8 ng/m^3 in April) and the lowest value in the monsoon season (88.5 ± 29.8 ng/m^3).

Average daily BC concentration was equal to 298.8 ± 341.3 ng/m^3, with a maximum in the pre-monsoon season (2772.3 ng/m^3) and a minimum in the monsoon season (36.4 ng/m^3). The diurnal variation of BC concentrations in the pre-monsoon season showed significant high values from mid-night to noon, and there was an increasing trend in the afternoon during the non-monsoon periods, implying the potential origin of BC are from the long-range transport. BC concentrations appeared two peaks in the morning and after the noon during the monsoon period, might be affected by the local anthropogenic activities.

The seasonal cycle of BC concentrations at QOMS was closely correlated with the variation of atmospheric circulation and combustion emissions in South Asia. In the non-monsoon seasons, affected by westerly, the air masses in the Mt. Everest region were largely from Pakistan, northern Indian, and Nepal, where existed high loading emissions of vegetation fires. In the monsoon season, the southerly winds were dominated in the Mt. Everest region and the air masses were mainly from the Arabian Sea and the Bay of Bengal. Under intense precipitation scavenging of BC and extremely low level of the combustion emissions in South Asia, BC concentrations at QOMS were close to the background level in the monsoon season.

For four heavy pollution episodes occurred at QOMS with BC concentrations above 1000 ng/m^3, we found that the transport processes of BC aerosols from South Asia to the Mt. Everest region were different as seasons varying. In the monsoon season (take the pollution event during 8-10 June 2015 as an example), BC aerosols were efficiently driven upward by the cyclone in the lower atmosphere in South Asia and transported to the Mt. Everest region by the southward winds in the upper atmosphere. However, during the pre-monsoon season (take the other three pollution events as example), the mountain-valley wind played an import role in the BC aerosols cross the Himalayas and were transported to the Mt. Everest region.

Data availability. All data are available upon requests made to the corresponding author.

Competing interests. The authors declare that they have no conflict of interest.

Special issue statement. This article is part of the special issue "Study of ozone, aerosols and radiation over the Tibetan Plateau (SOAR-TP) (ACP/AMT inter-journal SI)". It is not associated with a conference.

Acknowledgments. This study was supported by the National Nature Science Foundation of China (41630754, 41675130, 41421061), State Key Laboratory of Cryospheric Science (SKLCS-ZZ-2017). The authors thank the staff of the Qomolangma Atmospheric and Environmental Observation and Research Station of Chinese Academy of Sciences for collecting data and the support of meteorological dataset. We also give thanks to Tony Hansen for his suggestion on data processing and Xin Wan, Lekhendra Tripathee, and Yajun Liu for their help to improve the quality of this paper.

References

Anenberg, S. C., Schwartz, J., Shindell, D., Amann, M., Faluvegi, G., Klimont, Z., Janssens-Maenhout, G., Pozzoli, L., Van Dingenen, R., Vignati, E., Emberson, L., Muller, N. Z., West, J. J., Williams, M., Demkine, V., Hicks, W. K., Kuylenstierna, J., Raes, F., and Ramanathan, V.: Global air quality and health co-benefits of mitigating near-term climate change through methane and black carbon emission controls, Environ. Health Perspect., 120, 831-839, http://doi.org/10.1289/ehp.1104301, 2012.

Bonasoni, P., Laj, P., Angelini, F., Arduini, J., Bonafe, U., Calzolari, F., Cristofanelli, P., Decesari, S., Facchini, M. C., Fuzzi, S., Gobbi, G. P., Maione, M., Marinoni, A., Petzold, A., Roccato, F., Roger, J. C., Sellegri, K., Sprenger, M., Venzac, H., Verza, G. P., Villani, P., and Vuillermoz, E.: The ABC-Pyramid Atmospheric Research Observatory in Himalaya for aerosol, ozone and halocarbon measurements, Sci. Total Environ., 391, 252-261, http://doi.org/10.1016/j.scitotenv.2007.10.024, 2008.

Bond, T. C.: A technology-based global inventory of black and organic carbon emissions from combustion, J. Geophys. Res., 109, http://doi.org/10.1029/2003jd003697, 2004.

Bond, T. C., Doherty, S. J., Fahey, D. W., Forster, P. M., Berntsen, T., DeAngelo, B. J., Flanner, M. G., Ghan, S., Kärcher, B., Koch, D., Kinne, S., Kondo, Y., Quinn, P. K., Sarofim, M. C., Schultz, M. G., Schulz, M., Venkataraman, C., Zhang, H., Zhang, S., Bellouin, N., Guttikunda, S. K., Hopke, P. K., Jacobson, M. Z., Kaiser, J. W., Klimont, Z., Lohmann, U., Schwarz, J. P., Shindell, D., Storelvmo, T., Warren, S. G., and Zender, C. S.: Bounding the role of black carbon in the climate system: A scientific assessment, J. Geophys. Res.: Atmos., 118, 5380-5552, http://doi.org/10.1002/jgrd.50171, 2013.

Cao, J., Xu, B., He, J., Liu, X., Han, Y., Wang, G., and Zhu, C.: Concentrations, seasonal variations, and transport of carbonaceous aerosols at a remote Mountainous region in western China, Atmos. Environ., 43, 4444-4452, http://doi.org/10.1016/j.atmosenv.2009.06.023, 2009.

Chen, X., Su, Z., Ma, Y., and Sun, F.: Analysis of Land-Atmosphere Interactions over the North Region of Mt. Qomolangma (Mt. Everest), Arct. Antarct. Alp. Res., 44, 412-422, 2012.

Cong, Z., Kang, S., Kawamura, K., Liu, B., Wan, X., Wang, Z., Gao, S., and Fu, P.: Carbonaceous aerosols on the south edge of the Tibetan Plateau: concentrations, seasonality and sources, Atmos. Chem. Phys., 15, 1573-1584, http://doi.org/10.5194/acp-15-1573-2015, 2015a.

Cong, Z., Kawamura, K., Kang, S., and Fu, P.: Penetration of biomass-burning emissions from South Asia through the Himalayas: new insights from atmospheric organic acids, Sci. Rep., 5, 9580, http://doi.org/10.1038/srep09580, 2015b.

Cooke, W. F., Ramaswamy, V., and Kasibhatla, P.: A general circulation model study of the global carbonaceous aerosol distribution, J. Geophys. Res.: Atmos., 107, ACH 2-1-ACH 2-32, http://doi.org/10.1029/2001JD001274, 2002.

Dhungel, S., Kathayat, B., Mahata, K., and Panday, A.: Transport of regional pollutants through a remote trans-Himalayan

valley in Nepal, Atmos. Chem. Phys., 18, 1203-1216, http://doi.org/10.5194/acp-18-1203-2018, 2018.

Drinovec, L., Močnik, G., Zotter, P., Prévôt, A. S. H., Ruckstuhl, C., Coz, E., Rupakheti, M., Sciare, J., Müller, T., Wiedensohler, A., and Hansen, A. D. A.: The "dual-spot" Aethalometer: an improved measurement of aerosol black carbon with real-time loading compensation, Atmos. Meas. Tech., 7, 10179-10220, http://doi.org/10.5194/amtd-7-10179-2014, 2014.

Emmons, L. K., Walters, S., Hess, P. G., Lamarque, J. F., Pfister, G. G., Fillmore, D., Granier, C., Guenther, A., Kinnison, D., Laepple, T., Orlando, J., Tie, X., Tyndall, G., Wiedinmyer, C., Baughcum, S. L., and Kloster, S.: Description and evaluation of the Model for Ozone and Related chemical Tracers, version 4 (MOZART-4), Geosci. Model Dev., 3, 43-67, http://doi.org/10.5194/gmd-3-43-2010, 2010.

Fialho, P., Hansen, A. D. A., and Honrath, R. E.: Absorption coefficients by aerosols in remote areas: a new approach to decouple dust and black carbon absorption coefficients using seven-wavelength Aethalometer data, J. Aerosol Sci., 36, 267-282, http://doi.org/10.1016/j.jaerosci.2004.09.004, 2005.

Gao, X., Shi, Y., Song, R., Giorgi, F., Wang, Y., and Zhang, D.: Reduction of future monsoon precipitation over China: comparison between a high resolution RCM simulation and the driving GCM, Meteorol. Atmos. Phys., 100, 73-86, http://doi.org/10.1007/s00703-008-0296-5, 2008.

Grell, G. A., Peckham, S. E., Schmitz, R., McKeen, S. A., Frost, G., Skamarock, W. C., and Eder, B.: Fully coupled "online" chemistry within the WRF model, Atmos. Environ., 39, 6957-6975, http://doi.org/10.1016/j.atmosenv.2005.04.027, 2005.

Hansen, A. D. A., Rosen, H., and Novakov, T.: The aethalometer — An instrument for the real-time measurement of optical absorption by aerosol particles, Sci. Total Environ., 36, 191-196, http://doi.org/10.1016/0048-9697(84)90265-1, 1984.

Hansen, J., Sato, M., Ruedy, R., Lacis, A., and Oinas, V.: Global warming in the twenty-first century: An alternative scenario, Proc. Natl. Acad. Sci. U. S. A., 97, 9875-9880, http://doi.org/10.1073/pnas.170278997, 2000.

He, C., Li, Q. B., Liou, K. N., Zhang, J., Qi, L., Mao, Y., Gao, M., Lu, Z., Streets, D. G., Zhang, Q., Sarin, M. M., and Ram, K.: A global 3-D CTM evaluation of black carbon in the Tibetan Plateau, Atmos. Chem. Phys., 14, 7091-7112, http://doi.org/10.5194/acp-14-7091-2014, 2014.

Jacobson, M.: Control of fossil-fuel particulate black carbon and organic matter, possibly the most effective method of slowing global warming, J. Geophys. Res., 107, http://doi.org/10.1029/2001JD001376, 2002.

Jacobson, M. Z.: Strong radiative heating due to the mixing state of black carbon in atmospheric aerosols, Nature, 409, 695-697, http://doi.org/10.1038/35055518, 2001.

Ji, Z., Kang, S., Cong, Z., Zhang, Q., and Yao, T.: Simulation of carbonaceous aerosols over the Third Pole and adjacent regions: distribution, transportation, deposition, and climatic effects, Clim. Dyn., 45, 2831-2846, http://doi.org/10.1007/s00382-015-2509-1, 2015.

Ji, Z.: Modeling black carbon and its potential radiative effects over the Tibetan Plateau, Adv. Clim. Change. Res., 7, 139-144, http://doi.org/10.1016/j.accre.2016.10.002, 2016.

Jurado, E., Dachs, J., Duarte, C. M., and Simó, R.: Atmospheric deposition of organic and black carbon to the global oceans, Atmos. Environ., 42, 7931-7939, http://doi.org/10.1016/j.atmosenv.2008.07.029, 2008.

Kang, S., Xu, Y., You, Q., Fluegel, W.-A., Pepin, N., and Yao, T.: Review of climate and cryospheric change in the Tibetan Plateau, Environ. Res. Lett., 5, 015101, http://doi.org/10.1088/1748-9326/5/1/015101, 2010.

Kang, S., Chen, P., Li, C., Liu, B., and Cong, Z.: Atmospheric Aerosol Elements over the Inland Tibetan Plateau: Concentration, Seasonality, and Transport, Aerosol Air Qual. Res., 16, 789-800, http://doi.org/10.4209/aaqr.2015.05.0307, 2016.

Kopacz, M., Mauzerall, D. L., Wang, J., Leibensperger, E. M., Henze, D. K., and Singh, K.: Origin and radiative forcing of black carbon transported to the Himalayas and Tibetan Plateau, Atmos. Chem. Phys., 11, 2837-2852, http://doi.org/10.5194/acp-11-2837-2011, 2011.

Li, C., Chen, P., Kang, S., Yan, F., Hu, Z., Qu, B., and Sillanpää, M.: Concentrations and light absorption characteristics of carbonaceous aerosol in PM 2.5 and PM 10 of Lhasa city, the Tibetan Plateau, Atmos. Environ., 127, 340-346, http://doi.org/10.1016/j.atmosenv.2015.12.059, 2016.

Li, J. J., Wang, H. G., Wang, M. X., Cao, J. J., Sun, T., Cheng, C. L., Meng, J. J., Hu, T. F., and Liu, X. s.: Abundance, composition and source of atmospheric PM2.5 at a remote site in the Tibetan Plateau, China, Tellus Ser. B-Chem. Phys. Meteorol., 65, 20281, http://doi.org/10.3402/tellusb.v65i0.20281, 2013.

Li, X., Kang, S., He, X., Qu, B., Tripathee, L., Jing, Z., Paudyal, R., Li, Y., Zhang, Y., Yan, F., Li, G., and Li, C.: Light-absorbing impurities accelerate glacier melt in the Central Tibetan Plateau, Sci. Total Environ., 587, 482-490, http://doi.org/10.1016/j.scitotenv.2017.02.169, 2017.

Li, X., Kang, S., Zhang, G., Qu, B., Tripathee, L., Paudyal, R., Jing, Z., Zhang, Y., Yan, F., Li, G., Cui, X., Xu, R., Hu, Z., and Li, C.: Light-absorbing impurities in a southern Tibetan Plateau glacier: Variations and potential impact on snow albedo and radiative forcing, Atmos. Res., 200, 77-87, http://doi.org/10.1016/j.atmosres.2017.10.002, 2018.

Lu, A., Kang, S., Li, Z., and Theakstone, W. H.: Altitude effects of climatic variation on Tibetan Plateau and its vicinities, J. Earth Sci., 21, 189-198, http://doi.org/10.1007/s12583-010-0017-0, 2010.

Lu, Z., Streets, D. G., Zhang, Q., and Wang, S.: A novel back-trajectory analysis of the origin of black carbon transported to the Himalayas and Tibetan Plateau during 1996-2010, Geophys. Res. Lett., 39, L01809, http://doi.org/10.1029/2011gl049903, 2012.

Luthi, Z. L., Skerlak, B., Kim, S. W., Lauer, A., Mues, A., Rupakheti, M., and Kang, S.: Atmospheric brown clouds reach the Tibetan Plateau by crossing the Himalayas, Atmos. Chem. Phys., 15, 6007-6021, http://doi.org/10.5194/acp-15-6007-2015, 2015.

Ma, Y., Wang, Y., Zhong, L., Wu, R., Wang, S., and Li, M.: The Characteristics of Atmospheric Turbulence and Radiation Energy Transfer and the Structure of Atmospheric Boundary Layer over the Northern Slope Area of Himalaya, J. Meteorol. Soc. Jpn., 89A, 345-353, http://doi.org/10.2151/jmsj.2011-A24, 2011.

Marinoni, A., Cristofanelli, P., Laj, P., Duchi, R., Calzolari, F., Decesari, S., Sellegri, K., Vuillermoz, E., Verza, G. P., Villani, P., and Bonasoni, P.: Aerosol mass and black carbon concentrations, a two year record at NCO-P (5079 m, Southern Himalayas), Atmos. Chem. Phys., 10, 8551-8562, http://doi.org/10.5194/acp-10-8551-2010, 2010.

Menon, S., Koch, D., Beig, G., Sahu, S., Fasullo, J., and Orlikowski, D.: Black carbon aerosols and the third polar ice cap, Atmos. Chem. Phys., 10, 4559-4571, http://doi.org/10.5194/acp-10-4559-2010, 2010.

Ming, J., Cachier, H., Xiao, C., Qin, D., Kang, S., Hou, S., and Xu, J.: Black carbon record based on a shallow Himalayan ice core and its climatic implications, Atmos. Chem. Phys., 8, 1343-1352, http://doi.org/10.5194/acp-8-1343-2008, 2008.

Oshima, N., Kondo, Y., Moteki, N., Takegawa, N., Koike, M., Kita, K., Matsui, H., Kajino, M., Nakamura, H., Jung, J. S., and Kim, Y. J.: Wet removal of black carbon in Asian outflow: Aerosol Radiative Forcing in East Asia (A-FORCE) aircraft campaign, J. Geophys. Res., 117, D03204, http://doi.org/10.1029/2011jd016552, 2012.

Praveen, P. S., Ahmed, T., Kar, A., Rehman, I. H., and Ramanathan, V.: Link between local scale BC emissions and large scale atmospheric solar absorption, Atmos. Chem. Phys., 12, 1173-1187, http://doi.org/10.5194/acp-12-1173-2012, 2012.

Qu, B., Ming, J., Kang, S.-C., Zhang, G.-S., Li, Y.-W., Li, C.-D., Zhao, S.-Y., Ji, Z.-M., and Cao, J.-J.: The decreasing albedo of Zhadang glacier on western Nyainqentanglha and the role of light-absorbing impurities, Atmos. Chem. Phys., 14, 11117-11128, http://doi.org/10.5194/acp-14-11117-2014, 2014.

Ram, K., Sarin, M. M., and Hegde, P.: Long-term record of aerosol optical properties and chemical composition from a high-altitude site (Manora Peak) in Central Himalaya, Atmos. Chem. Phys., 10, 11791-11803, http://doi.org/10.5194/acp-10-11791-2010, 2010.

Ramanathan, V., Chung, C., Kim, D., Bettge, T., Buja, L., Kiehl, J. T., Washington, W. M., Fu, Q., Sikka, D. R., and Wild, M.: Atmospheric brown clouds: impacts on South Asian climate and hydrological cycle, P. Natl. Acad. Sci. USA, 102, 5326-5333, http://doi.org/10.1073/pnas.0500656102, 2005.

Ramanathan, V., and Ramana, M. V.: Persistent, Widespread, and Strongly Absorbing Haze Over the Himalayan Foothills and the Indo-Gangetic Plains, Pure appl. geophys., 162, 1609-1626, http://doi.org/10.1007/s00024-005-2685-8, 2005.

Ramanathan, V., and Carmichael, G.: Global and Regional Climate Changes Due to Black Carbon, Nature Geosci., 1, 221-227, http://doi.org/10.1038/ngeo156, 2008.

Sandradewi, J., Prevot, A., Szidat, S., Perron, N., Alfarra, M., A Lanz, V., Weingartner, E., and Baltensperger, U.: Using aerosol light absorption measurements for the quantitative determination of wood burning and traffic emission contributions to particulate matter, Environ. Sci. Technol., 42, 3316-3323, http://doi.org/10.1021/es702253m, 2008a.

Sandradewi, J., Prevot, A., Weingartner, E., Schmidhauser, R., Gysel, M., and Baltensperger, U.: A study of wood burning and traffic aerosols in an Alpine valley using a multi-wavelength Aethalometer, Atmos. Environ., 42, 101-112, http://doi.org/10.1016/j.atmosenv.2007.09.034, 2008b.

Skamarock, W. C., Klemp, J. B., Dudhia, J., Gill, D. O., Barker, D. M., Wang, W., and Powers, J. G.: A Description of the

Advanced Research WRF Version 2, NCAR Technical Note NCAR/TN-468+STR, http://doi.org/doi:10.5065/D6DZ069T, 2005.

Tripathee, L., Kang, S., Rupakheti, D., Cong, Z., Zhang, Q., and Huang, J.: Chemical characteristics of soluble aerosols over the central Himalayas: insights into spatiotemporal variations and sources, Environ. Sci. Pollut. Res., 24, 24454-24472, http://doi.org/10.1007/s11356-017-0077-0, 2017.

Vadrevu, K. P., Ellicott, E., Giglio, L., Badarinath, K. V. S., Vermote, E., Justice, C., and Lau, W. K. M.: Vegetation fires in the himalayan region – Aerosol load, black carbon emissions and smoke plume heights, Atmos. Environ., 47, 241-251, http://doi.org/10.1016/j.atmosenv.2011.11.009, 2012.

Wan, X., Kang, S., Wang, Y., Xin, J., Liu, B., Guo, Y., Wen, T., Zhang, G., and Cong, Z.: Size distribution of carbonaceous aerosols at a high-altitude site on the central Tibetan Plateau (Nam Co Station, 4730ma.s.l.), Atmos. Res., 153, 155-164, http://doi.org/10.1016/j.atmosres.2014.08.008, 2015.

Wang, M., Xu, B., Wang, N., Cao, J., Tie, X., Wang, H., Zhu, C., and Yang, W.: Two distinct patterns of seasonal variation of airborne black carbon over Tibetan Plateau, Sci. Total Environ., 573, 1041-1052, http://doi.org/10.1016/j.scitotenv.2016.08.184, 2016.

Wiedinmyer, C., Akagi, S. K., Yokelson, R. J., Emmons, L. K., Al-Saadi, J. A., Orlando, J. J., and Soja, A. J.: The Fire INventory from NCAR (FINN): a high resolution global model to estimate the emissions from open burning, Geosci. Model Dev., 4, 625-641, http://doi.org/10.5194/gmd-4-625-2011, 2011.

Wu, G., Xu, B., Zhang, C., and Gao, S.: Atmospheric dust aerosols over the Eastern Pamirs: major element concentrations and composition, Environ. Earth Sci., 61, 1227-1237, http://doi.org/10.1007/s12665-009-0446-1, 2010.

Xu, B.-Q., Wang, M., Joswiak, D. R., Cao, J.-J., Yao, T.-D., Wu, G.-J., Yang, W., and Zhao, H.-B.: Deposition of anthropogenic aerosols in a southeastern Tibetan glacier, J. Geophys. Res., 114, D17209, http://doi.org/10.1029/2008JD011510, 2009.

Xu, C., Ma, Y. M., Panday, A., Cong, Z. Y., Yang, K., Zhu, Z. K., Wang, J. M., Amatya, P. M., and Zhao, L.: Similarities and differences of aerosol optical properties between southern and northern sides of the Himalayas, Atmos. Chem. Phys., 14, 3133-3149, http://doi.org/10.5194/acp-14-3133-2014, 2014.

Xu, Y., Ramanathan, V., and Washington, W. M.: Observed high-altitude warming and snow cover retreat over Tibet and the Himalayas enhanced by black carbon aerosols, Atmos. Chem. Phys., 16, 1303-1315, http://doi.org/10.5194/acp-16-1303-2016, 2016.

Yang, J., Duan, K., Kang, S., Shi, P., and Ji, Z.: Potential feedback between aerosols and meteorological conditions in a heavy pollution event over the Tibetan Plateau and Indo-Gangetic Plain, Clim. Dyn., 48, 2901-2917, http://doi.org/10.1007/s00382-016-3240-2, 2017.

Yang, J., Kang, S., Ji, Z., and Chen, D.: Modeling the Origin of Anthropogenic Black Carbon and Its Climatic Effect Over the Tibetan Plateau and Surrounding Regions, J. Geophys. Res.: Atmos., n/a-n/a, http://doi.org/10.1002/2017JD027282, 2018.

Yang, M., Howell, S. G., Zhuang, J., and Huebert, B. J.: Attribution of aerosol light absorption to black carbon, brown carbon, and dust in China - interpretations of atmospheric measurements during EAST-AIRE, Atmos. Chem. Phys., 9, 2035-2050, http://doi.org/10.5194/acp-9-2035-2009, 2009.

Yang, S., Xu, B., Cao, J., Zender, C. S., and Wang, M.: Climate effect of black carbon aerosol in a Tibetan Plateau glacier, Atmos. Environ., 111, 71-78, http://doi.org/10.1016/j.atmosenv.2015.03.016, 2015.

Yao, T., Thompson, L. G., Mosbrugger, V., Zhang, F., Ma, Y., Luo, T., Xu, B., Yang, X., Joswiak, D. R., Wang, W., Joswiak, M. E., Devkota, L. P., Tayal, S., Jilani, R., and Fayziev, R.: Third Pole Environment (TPE), Environ. Dev., 3, 52-64, http://doi.org/10.1016/j.envdev.2012.04.002, 2012.

Yasunari, T. J., Bonasoni, P., Laj, P., Fujita, K., Vuillermoz, E., Marinoni, A., Cristofanelli, P., Duchi, R., Tartari, G., and Lau, K. M.: Estimated impact of black carbon deposition during pre-monsoon season from Nepal Climate Observatory – Pyramid data and snow albedo changes over Himalayan glaciers, Atmos. Chem. Phys., 10, 6603-6615, http://doi.org/10.5194/acp-10-6603-2010, 2010.

Zhang, Q., Streets, D. G., Carmichael, G. R., He, K. B., Huo, H., Kannari, A., Klimont, Z., Park, I. S., Reddy, S., Fu, J. S., Chen, D., Duan, L., Lei, Y., Wang, L. T., and Yao, Z. L.: Asian emissions in 2006 for the NASA INTEX-B mission, Atmos. Chem. Phys., 9, 5131-5153, http://doi.org/10.5194/acp-9-5131-2009, 2009.

Zhang, R., Wang, H., Qian, Y., Rasch, P. J., Easter, R. C., Ma, P. L., Singh, B., Huang, J., and Fu, Q.: Quantifying sources, transport, deposition, and radiative forcing of black carbon over the Himalayas and Tibetan Plateau, Atmos. Chem. Phys., 15, 6205-6223, http://doi.org/10.5194/acp-15-6205-2015, 2015.

Zhang, X., Ming, J., Li, Z., Wang, F., and Zhang, G.: The online measured black carbon aerosol and source orientations in the Nam Co region, Tibet, Environ. Sci. Pollut. Res., 24, 25021-25033, http://doi.org/10.1007/s11356-017-0165-1, 2017a.

Zhang, Y., Kang, S., Cong, Z., Schmale, J., Sprenger, M., Li, C., Yang, W., Gao, T., Sillanpää, M., Li, X., Liu, Y., Chen, P., and Zhang, X.: Light-absorbing impurities enhance glacier albedo reduction in the southeastern Tibetan plateau, J. Geophys. Res.: Atmos., 122, 6915-6933, http://doi.org/10.1002/2016JD026397, 2017b.

Zhao, S., Ming, J., Xiao, C., Sun, W., and Qin, X.: A preliminary study on measurements of black carbon in the atmosphere of northwest Qilian Shan, J. Environ. Sci., 24, 152-159, http://doi.org/10.1016/s1001-0742(11)60739-0, 2012.

Zou, H., Zhou, L., Ma, S., Li, P., Wang, W., Li, A., Jia, J., and Gao, D.: Local wind system in the Rongbuk Valley on the northern slope of Mt. Everest, Geophys. Res. Lett., 35, L13813, http://doi.org/10.1029/2008gl033466, 2008.

Table 1. Mean BC concentrations at QOMS and compared with other remote sites.

Name	Location	Sample	Sampling period	BC or EC (ng/m^3)	Reference
QOMS	Southern TP (28.36°N, 86.95°E, 4276m)	AE33	May 2015-Apr 2016	298.8 ± 341.3	This paper
QOMS	Southern TP (28.36°N, 86.95°E, 4276m)	TSP	Aug 2009-Jul 2010	250 ± 220	Cong et al. (2015)
Ranwu	Southeast TP (29.32°N, 96.96°E, 4600m)	AE31	Nov 2012-Jun 2013	139.1	Wang et al. (2016)
Lhasa	Southwest TP (29.65°N, 91.03°E, 3642m)	PM 10	May 2013-Mar 2014	2310	Li et al. (2016)
Nam Co	Central TP (30.46°N, 90.59°E, 4730m)	TSP	Jan-Dec 2012	190	Wan et al. (2015)
Qilianshan	Northern TP (39.50°N, 96.51°E, 4214m)	AE31	May 2009-Mar 2011	48	Zhao et al. (2012)
Qinghai Lake	Northeast TP (37.00°N, 99.90°E, 3200m)	PM 2.5	Jul-Aug 2010	370	Li et al. (2013)
Muztagh Ata	Northwest TP (38.29°N, 75.02°E, 4500m)	TSP	Dec 2003-Feb 2006	55	Cao et al. (2009)
NCO-P, Nepal	Southern Himalayas (27.95°N, 86.82°E, 5079m)	PM 1	Mar 2006-Feb 2008	160.5 ±296.1	Marinoni et al. (2010)
Manora Peak, India	Central Himalayas (29.40° N, 79.50° E, 1950m)	TSP	Feb 2005–Jul 2008	In the range of 140-7600	Ram et al. (2010)

Atmos. Chem. Phys. Discuss., https://doi.org/10.5194/acp-2018-183
Manuscript under review for journal Atmos. Chem. Phys.
Discussion started: 9 March 2018

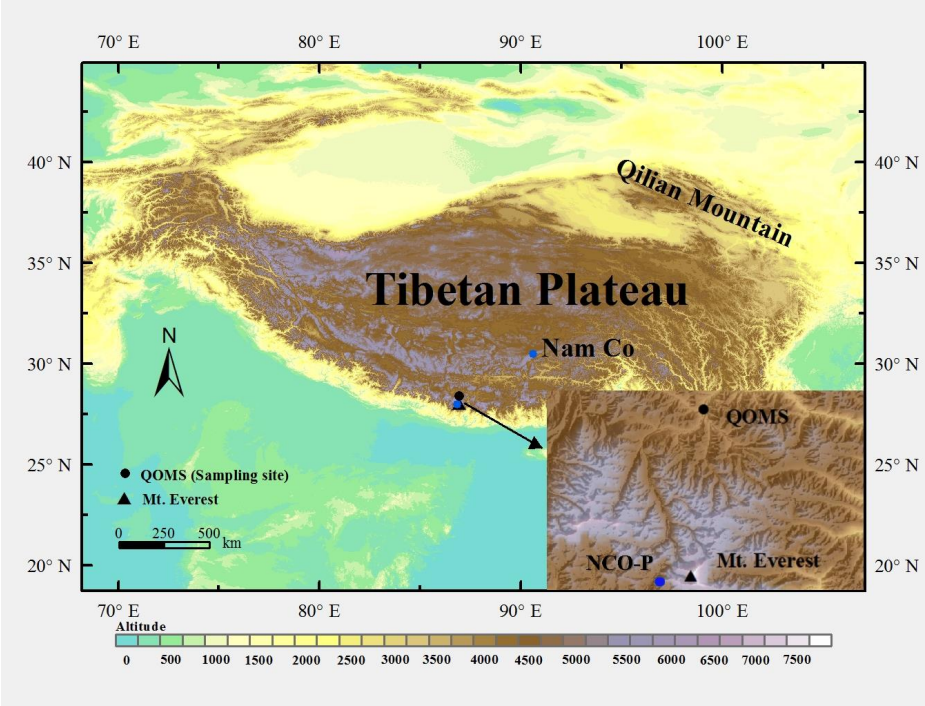

Figure 1: Location of the sampling site.

Atmos. Chem. Phys. Discuss., https://doi.org/10.5194/acp-2018-183
Manuscript under review for journal Atmos. Chem. Phys.
Discussion started: 9 March 2018

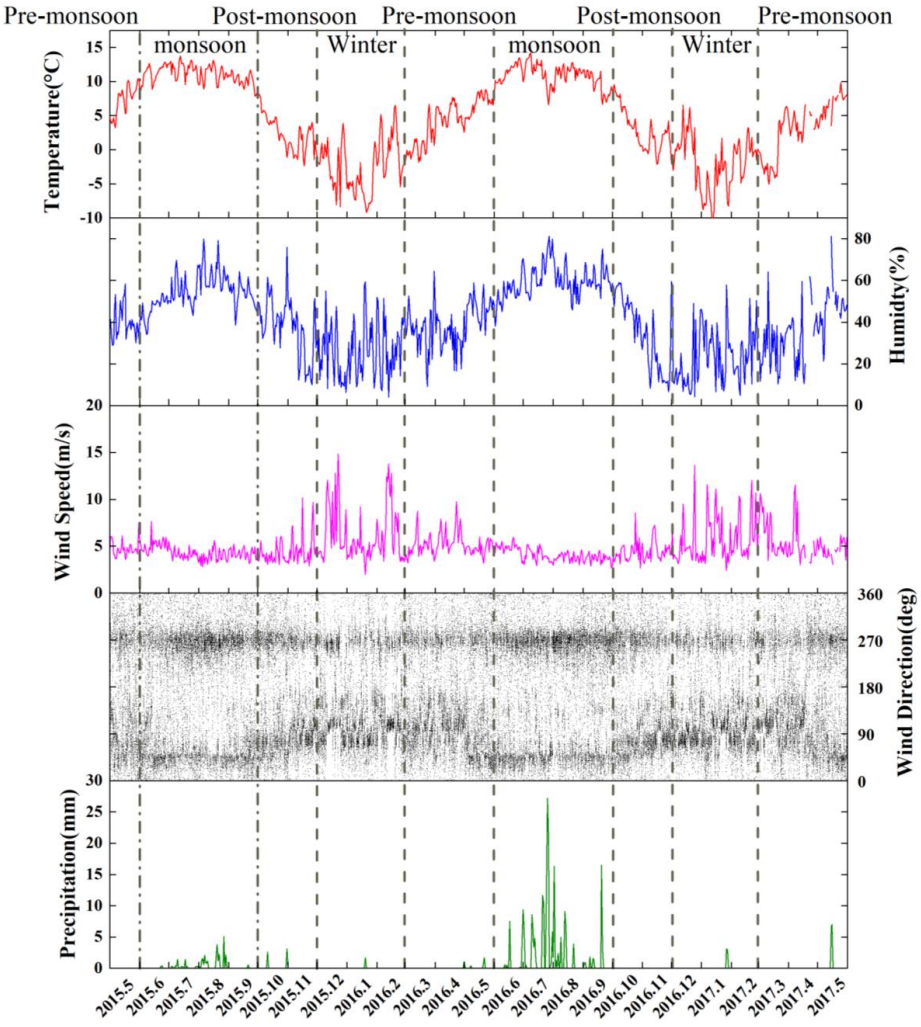

Figure 2: Variations of temperature, humidity, wind speed, wind direction, and precipitation at QOMS from May 2015 to May 2017.

Atmos. Chem. Phys. Discuss., https://doi.org/10.5194/acp-2018-183
Manuscript under review for journal Atmos. Chem. Phys.
Discussion started: 9 March 2018

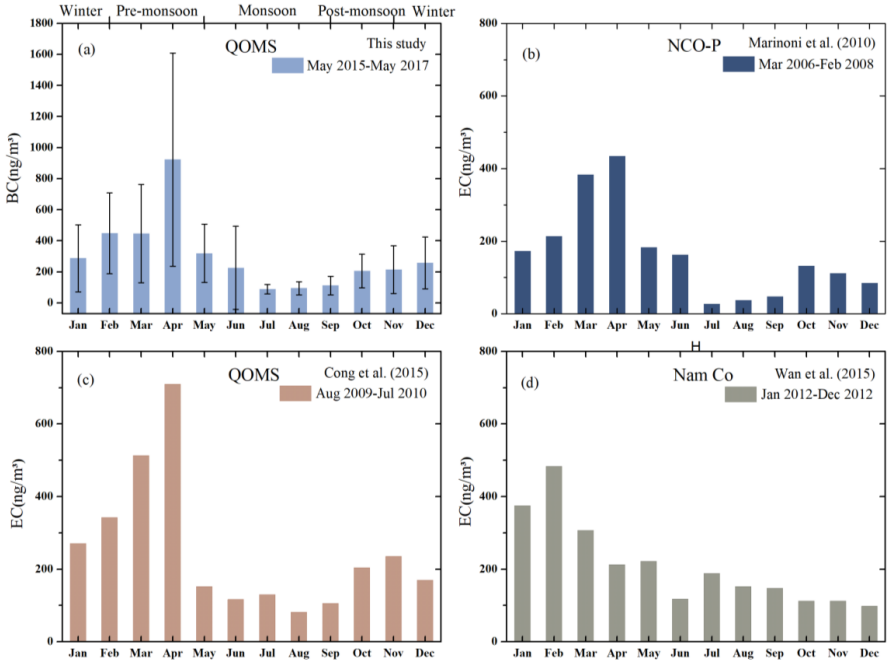

Figure 3: (a) Monthly mean BC concentrations at QOMS from May 2015 to May 2017 in this study; (b) Monthly mean EC at NCO-P from March 2006 to February 2008 from Marinoni et al. (2010); (c) Monthly mean EC at QOMS from August 2009 to July 2010 from Cong et al. (2015); (d) Monthly mean EC at Nam Co station from January to December 2012 from Wan et al. (2015).

Atmos. Chem. Phys. Discuss., https://doi.org/10.5194/acp-2018-183
Manuscript under review for journal Atmos. Chem. Phys.
Discussion started: 9 March 2018

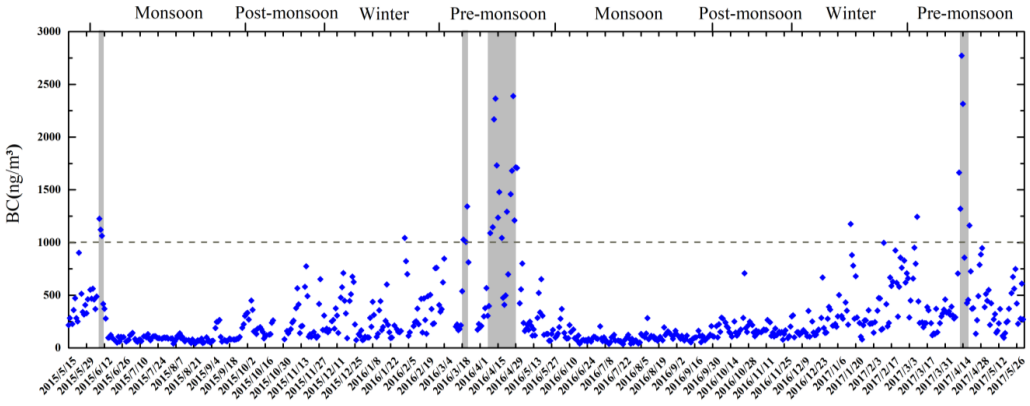

Figure 4: Daily mean BC concentrations at QOMS during study period (the gray bars represent the continuous high values more than 1000 ng/m^3).

Atmos. Chem. Phys. Discuss., https://doi.org/10.5194/acp-2018-183
Manuscript under review for journal Atmos. Chem. Phys.
Discussion started: 9 March 2018

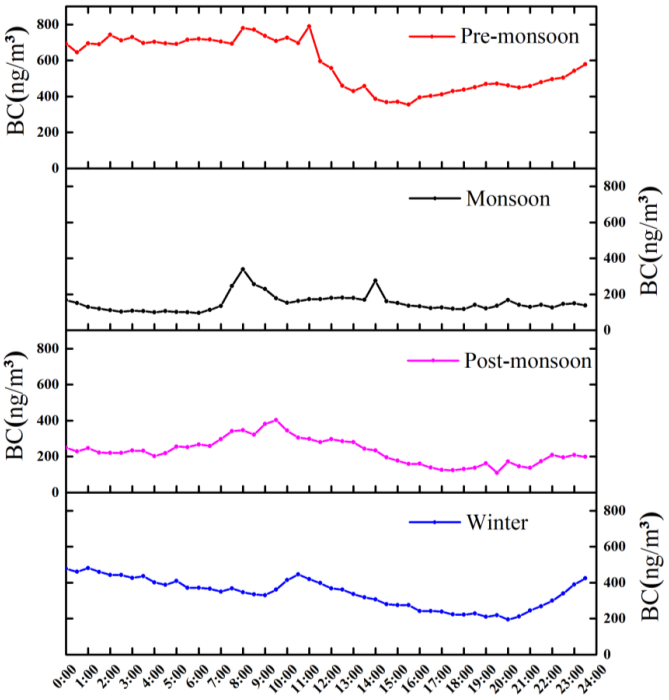

Figure 5: Diurnal variation of BC concentrations (every half an hour) at QOMS during study period.

Atmos. Chem. Phys. Discuss., https://doi.org/10.5194/acp-2018-183
Manuscript under review for journal Atmos. Chem. Phys.
Discussion started: 9 March 2018

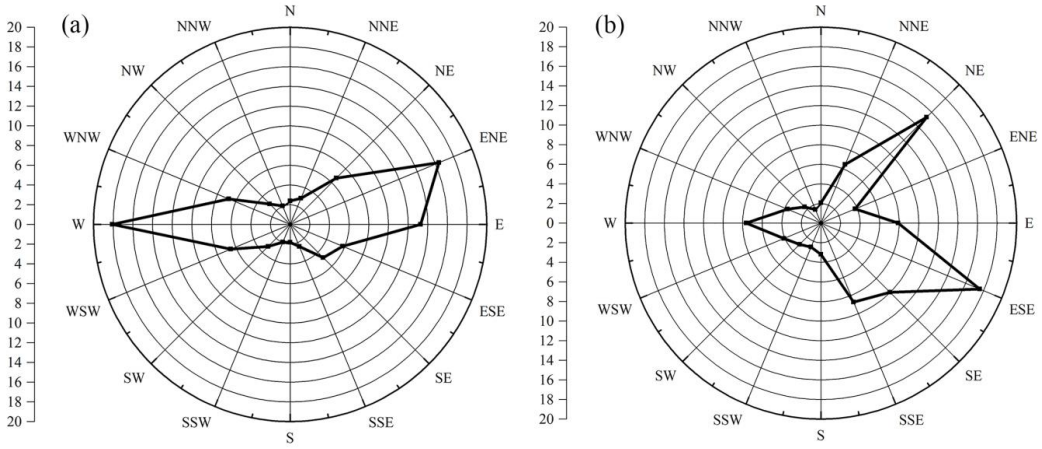

Figure 6. Wind direction frequency at QOMS in the pre-monsoon season (a) 0:00-12:00; (b) 12:00-24:00.

Atmos. Chem. Phys. Discuss., https://doi.org/10.5194/acp-2018-183
Manuscript under review for journal Atmos. Chem. Phys.
Discussion started: 9 March 2018

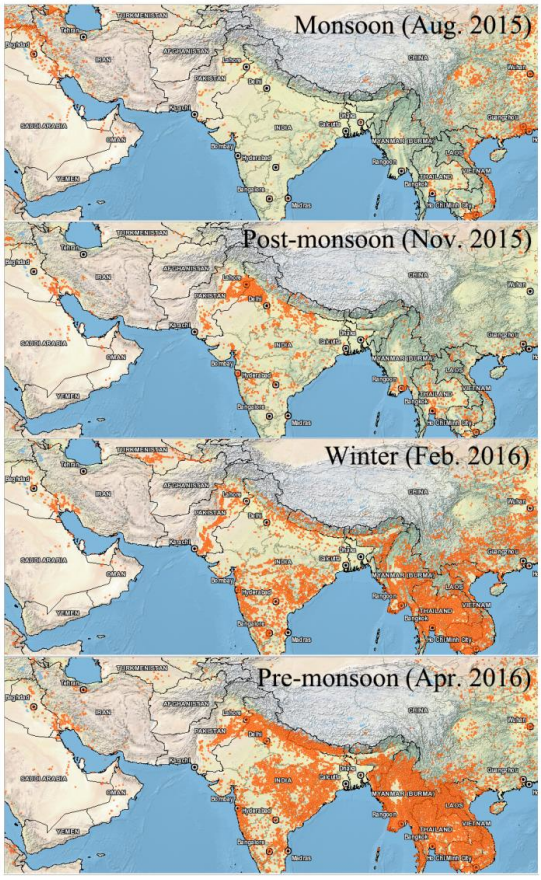

Figure 7. The distribution of fire spots in different seasons from August 2015 to April 2016.

Atmos. Chem. Phys. Discuss., https://doi.org/10.5194/acp-2018-183
Manuscript under review for journal Atmos. Chem. Phys.
Discussion started: 9 March 2018

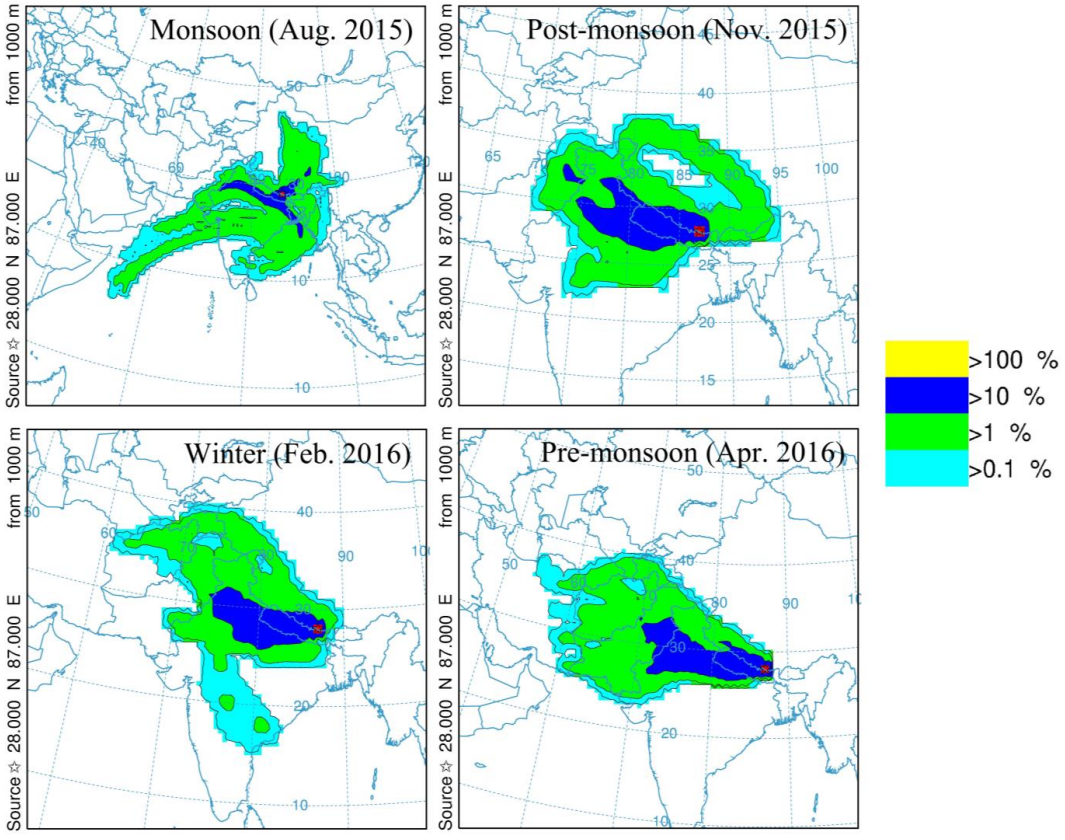

Figure 8. Frequency plots for 5-day back trajectories calculated by HYSPLIT model at QOMS in different seasons from August 2015 to April 2016.

Atmos. Chem. Phys. Discuss., https://doi.org/10.5194/acp-2018-183
Manuscript under review for journal Atmos. Chem. Phys.
Discussion started: 9 March 2018

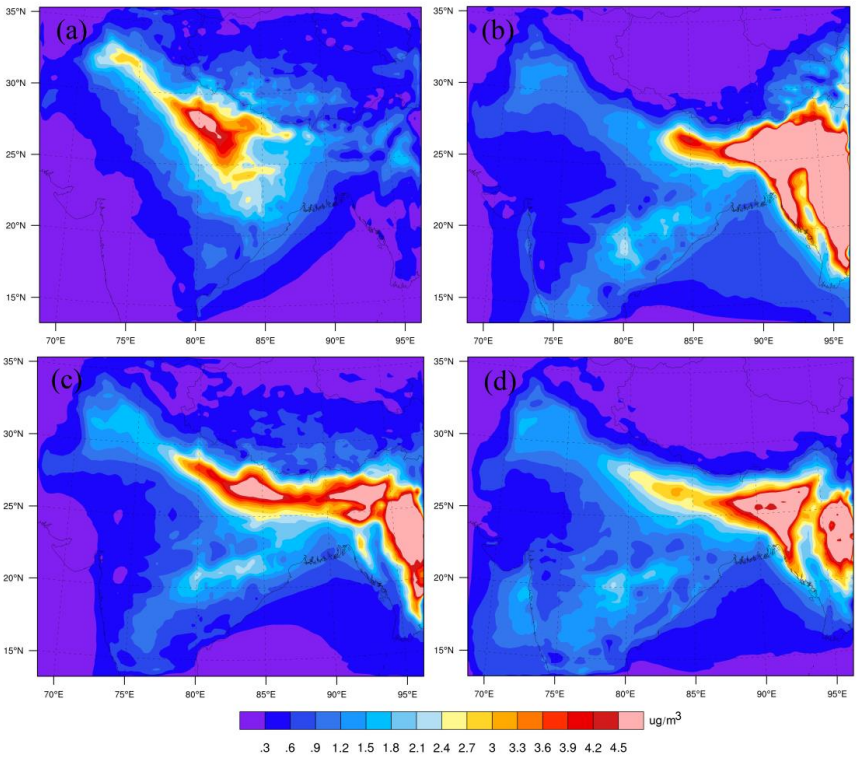

Figure 9. Mean BC concentration simulated by WRF-Chem model at QOMS and its vicinities: (a) event A; (b) event B; (c) event C; (d) event D.

Atmos. Chem. Phys. Discuss., https://doi.org/10.5194/acp-2018-183
Manuscript under review for journal Atmos. Chem. Phys.
Discussion started: 9 March 2018

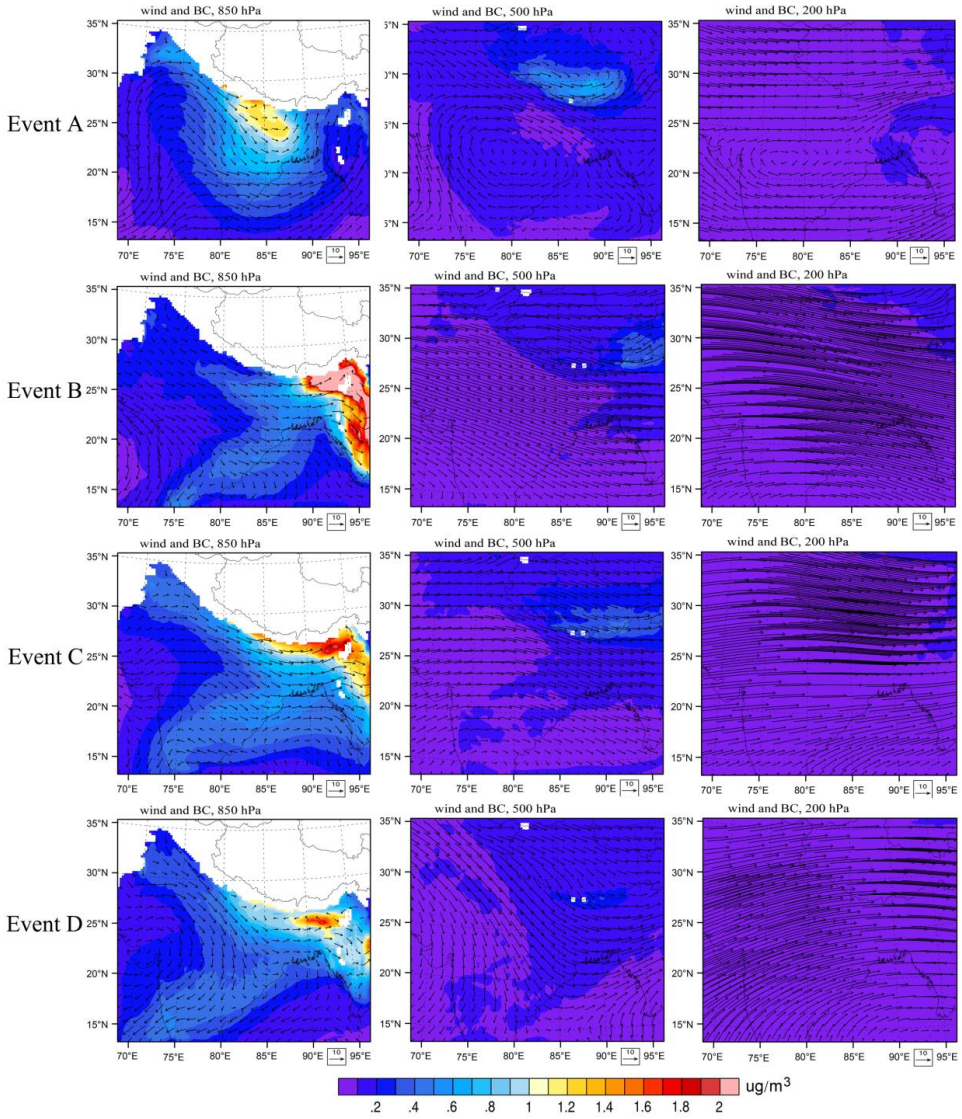

Figure 10. Mean BC concentration and wind at 850 hpa, 500 hpa, and 200 hpa simulated by WRF-Chem model at QOMS and its vicinities: event A (the first row); event B (the second row); event C (the third row); event D (the last row).

Atmos. Chem. Phys. Discuss., https://doi.org/10.5194/acp-2018-183
Manuscript under review for journal Atmos. Chem. Phys.
Discussion started: 9 March 2018

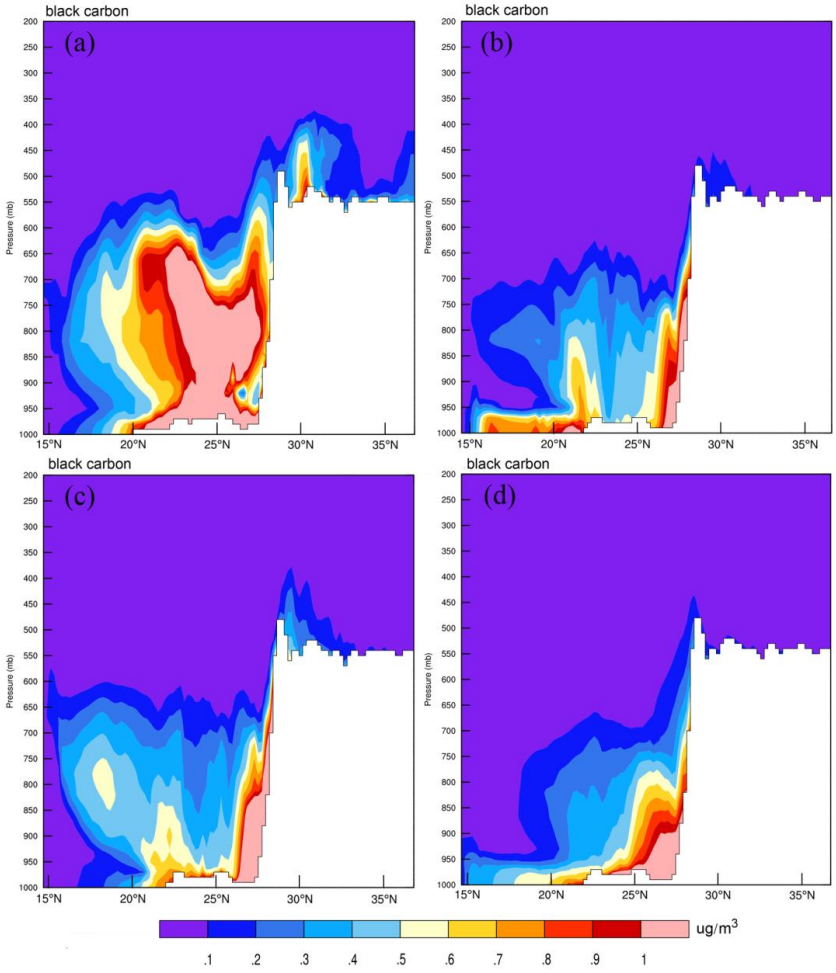

Figure 11. Vertical profiles of mean BC concentration among the QOMS's longitude of 86.95°E: (a) event A; (b) event B; (c) event C; (d) event D.